Preprints of the 19th World Congress
The International Federation of Automatic Control
Cape Town, South Africa. August 24-29, 2014

Fault condition recognition based on multi-scale co-occurrence matrix for copper flotation process

Lu Zhao*,Tao Peng*,Hua Han*, Wei Cao*, Yangge Lou*,Xiaotian Xie**

**School of Information Science and Engineering, Central South University, Changsha 410083*
***Harbin Institute of Technology, Harbin 150001*
China (e-mail: zhaolu1219@163.com, pandtao@163.com).

Abstract: Image processing technology has been successfully applied to fault detection of copper flotation processes, and the key to realize image processing based fault condition recognition is accurately extracting froth image features closely related to key production indices. To extract texture features of froth images in real-time, a multi-scale gray level co-occurrence matrix (M-GLCM) method is proposed. Firstly, the wavelet transform is applied to the froth gray images, and the coefficients of wavelet approximation sub-images in different scales are mapped into gray level of 0~255. Then the spatial gray level co-occurrence matrices are calculated, a set of texture features of froth images are obtained statistically from the matrices. Lastly, these features are adopted for off-line classification and on-line recognition of froth images in different working conditions. As the result shows, froth texture features extracted through the multi-scale gray level co-occurrence matrix have a good stability and separability suitable for mode classification and thus can be well applied for fault condition recognition in copper flotation processes.

Key words: *multi-scale gray level co-occurrence matrix (M-GLCM); texture feature extraction; froth image; fault condition recognition; copper flotation;*

1. INTRODUCTION

Visual features of froth play a critical role in flotation processes since they can effectively reflect quality index like flotation grade etc. (Moolman et al., 1996). In traditional practice, the current working condition of a flotation process is determined by the visual features of froth surface through the direct observation of experienced operators. With its great arbitrariness and lack of objectivity, the traditional way can hardly help to accurately determine the current working condition and guide the operation in flotation processes, which ultimately lead to a great volatility in product quality. Therefore, the rapid and accurate recognition of working conditions is crucial to the entire flotation process.

In recent years, much progress has been made in intelligent working condition recognition of flotation processes, in which froth image features are adopted together with machine vision and image processing technology (Aldrich C. et al., 2010). Froth image features adopted in intelligent recognition of flotation working conditions mainly include the color, size, texture, etc. of froth (Yang et al., 2009; Xu et al., 2012; Lin et al., 2013), among which the froth texture is one of the key features since it is relatively stable to the influence of environment and illuminance (Yang et al., 2011). At present, methods including gray level co-occurrence matrix (GLCM, Haralick et al., 1973) and wavelet transform (Mallat, 1989) are most frequently cited for froth texture analysis. The GLCM are widely adopted based on second order statistics, since it is easily understood and rotational invariance. Based on GLCM, energy, entropy and inertia of froth image were extracted to characterize the froth appearance texture and to recognize flotation conditions in Wang et al. (2010) and Ren et al. (2011). These features can only reflect the spatial information of froth texture at a single scale, yet lacking of description on the dependency relationship between scales of froth texture (Liu et al., 2009). On the contrary, wavelet transform has the multi-scale property, which enables a combination of time-frequency domain for signal analysis, and thus performs better for identification with texture statistical features derived from it. The magnitude and phase spectra or the energy features of froth images were extracted by applying wavelet transform and then the minor differences of various types of froth under different flotation conditions were obtained in Liu et al.(2010) and Gianni B.et al.(2006). However, these statistical features only take the property of sub-band into account and ignore the structural information of froth texture. Zhong et al.(2011) have proposed a multi-resolution co-occurrence matrix by combining wavelet transform with spatial gray level co-occurrence matrix. The higher classification

accuracy of the features extracted by this new matrix was proved with a comparison among the features obtained by wavelet transform and GLCM. However, it has not been reported so far that M-GLCM were employed to extract texture features of froth images and recognize fault working conditions in copper flotation processes.

In this paper, the multi-scale spatial gray level co-occurrence matrix (M-GLCM) is adopted for extraction of texture features from flotation froth images. Firstly, wavelet transform of froth images is carried out, and the coefficients in the wavelet sub-images at different scales are mapped to gray level of 0~255. Based on the statistics of the spatial gray level co-occurrence matrix, a set of texture features are obtained, which can effectively reflect the multi-scale textural information of froth images. Finally, these features are used for fault condition recognition in flotation.

2. FAULT CONDITION RECOGNITION SYSTEM FOR COPPER FLOTATION PROCESS

Fig.1 shows the recognition system for working condition in copper flotation. In this system, froth videos from flotation site are captured by cameras and the image data is pre-processed, after which features of froth images are extracted. Based on certain features, different types of froth images can be classified so as to realize the recognition of working condition in flotation.

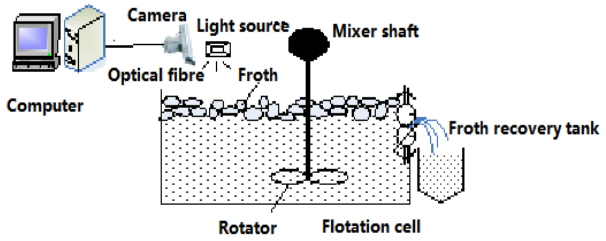

Fig.1 Sketch diagram of condition recognition system in copper flotation

As an important visual feature, froth texture can well reflect changes of key production indices and technological parameters in flotation process. Fig.2 and Fig.3 show respectively froth image under normal condition and that under fault condition from the copper flotation site. In normal condition, the froth is of relatively a rough texture and large size, with low spatial variation frequency of gray level; Under fault condition, the hydrated froths are mainly of a fine texture and small size, with high spatial variation frequency of gray level, while the viscous froths are of a relatively high viscosity and generally smaller than normal ones, with moderate spatial variation frequency of gray level.

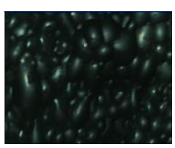

Fig.2 Froth image of normal condition

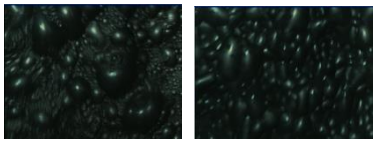

(a) Hydrated froth (b) Viscous froth

Fig.3 Froth images of fault conditions

By extracting froth features sensitive to the condition changes, fault conditions such as hydrated froth and viscous froth, etc. can be detected for timely adjustment of production operation and in this way, the copper flotation process can be kept at its optimal state. Since statistical features generated from GLCM can only describe the texture structural information on the spatial domain of images, which is obtained at a single scale, there is a loss of dependency relationship between texture scales. Wavelet analysis enables decomposition of original images into sub-band images of different frequencies or resolutions, in which the high-frequency sub-band reflects details of images such as texture, edge and so on, while the low-frequency sub-band reflects outline information of images. However, wavelet analysis is helpless for the analysis of structural information of froth texture. With the combination of wavelet analysis and GLCM, richer structural information of texture can be obtained.

3. TEXTURE FEATURE EXTRACTION OF FROTH IMAGE BASED ON GLCM

3.1 Gray Level Co-Occurrence Matrix

The GLCM shows the joint probability of the intensity values of two pixels i and j with a distance d apart along a certain direction θ, i.e., the probability that i and j have the same intensity. It can be shown by a matrix $P(i, j \mid d, \theta)$ as follow (Haralick et al., 1973):

$$P(i,j|d,\theta)=\left\{\left[(x,y),(x+\Delta x,y+\Delta y)\right]\middle| f(x,y)=i,\ f(x+\Delta x,y+\Delta y)=j,x=0,1,\cdots,M-1;\ y=0,1,\cdots,N-1\right\} \quad (1)$$

In formula (1) where $i, j = 0,1,\ldots L-1$, L is the quantization of image gray level; x and y are the horizontal and vertical coordinates of pixels in images; M and N represent respectively the number of rows and columns of images; θ is the included angle between the line from one pixel to the other and the positive x-axis, and is generally set at four discrete directions, namely, 0°, 45°, 90° and 135°, as shown in Fig.4. Moreover, $d=(\Delta x, \Delta y)$ and it is generally adopted 1, $\Delta x = d\cos\theta$ and $\Delta y = d\sin\theta$.

Since the number of quantitative series for image gray-level is set as an integer from 0 to $L-1$, P is a matrix with a $L \times L$ dimension in regard to a given d and θ.

Fig.5 shows the spatial gray-level co-occurrence matrix for

an image $f(x,y)$ when $\theta = 0°$ and $d = 1$.

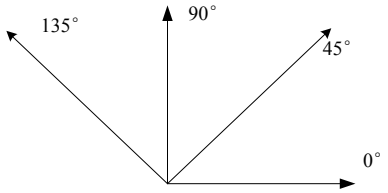

Fig.4 Four angles in spatial gray-level co-occurrence matrix

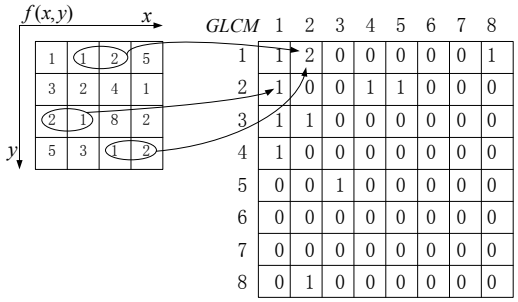

Fig.5 An example of spatial gray-level co-occurrence matrix

3.2 Multi-scale Spatial Gray-level Co-occurrence Matrix

3.2.1 Multi-scale Wavelet Analysis

Image texture generally has a multi-scale property, which demonstrates different texture features in different scales. Accordingly, the multi-scale decomposition in wavelet transform meets the demand and thus offers an effective tool for the analysis of texture details at different scales. Therefore, the wavelet analysis is adopted for the multi-scale decomposition of images at first.

By graying the original RGB froth image, the gray-level image $\mathbf{I}_{(p\times q)}$ is obtained. The two-dimensional j -level wavelet decomposition of grayscale image $\mathbf{I}_{(p\times q)}$ (c^{j+1} as its coefficient matrix) is carried out; At each decomposition level, an approximation sub-image and three detail sub-images respectively on the horizontal, vertical and diagonal directions are obtained.

The wavelet transform formula at each decomposition level is as follows (Mallat, 1989):

$$I = \sum_{k,m} c_{k,m}^{j+1} \varphi_{j+1,k,m} = \sum_{k,m} c_{k,m}^{j} \varphi_{j,k,m} + \sum_{k,m} d_{k,m}^{j,1} \psi_{j,k,m}^{1} + \sum_{k,m} d_{k,m}^{j,2} \psi_{j,k,m}^{2} + \sum_{k,m} d_{k,m}^{j,3} \psi_{j,k,m}^{3} \quad (2)$$

At each decomposition level, an approximation coefficient matrix $c_{k,m}^{j}$ d three details coefficient matrices $d_{k,m}^{j,1}$, $d_{k,m}^{j,2}$ and $d_{k,m}^{j,3}$ can be obtained with the Mallat algorithm for two-dimensional wavelet decomposition, as shown in following formula:

$$\begin{cases} c_{k,m}^{j} = \sum_{l,n} \bar{h}_{2k-l} \bar{h}_{2m-n} c_{l,n}^{j+1} \\ d_{k,m}^{j,1} = \sum_{l,n} \bar{h}_{2k-l} \bar{g}_{2m-n} c_{l,n}^{j+1} \\ d_{k,m}^{j,2} = \sum_{l,n} \bar{g}_{2k-l} \bar{h}_{2m-n} c_{l,n}^{j+1} \\ d_{k,m}^{j,3} = \sum_{l,n} \bar{g}_{2k-l} \bar{g}_{2m-n} c_{l,n}^{j+1} \end{cases} \quad (3)$$

In formula (2), φ refers to the scale function, ψ the wavelet function and j the decomposition layers; $k,m \in Z$ represent respectively rows and columns in coefficient matrix $c_{k,m}^{j}$, and $l,n \in Z$ represent respectively rows and columns in coefficient matrix $c_{l,n}^{j+1}$; the coefficient sequence $h = \{h_i\}$ is a low-pass filter and $\bar{h} = \{\bar{h}_i\}$ is the sequential inversion of h, namely $\bar{h}_i = h_{-i}$, while the coefficient sequence $g = \{g_i\}$ is a high-pass filter and $g_i = (-1)^i h_{1-i}$, $\bar{g} = \{\bar{g}_i\}$ is the sequential inversion of g, namely $\bar{g}_i = g_{-i}$.

Formula (2) is firstly used for the 1st -level of two-dimensional wavelet transform to obtain an approximation sub-image and three detail sub-images, coefficients of which are calculated through formula (3); and then formula (2) is used for 2nd -level two-dimensional wavelet transform of the 1st-level approximation sub-image (low-frequency part) $c_{k,m}^{j}$, which produces a 2nd-level approximation sub-image and three detail sub-images; the process then is repeated till the wavelet transform of $c_{k,m}^{j+1}$ at j level is done and accordingly, the multi-scale representation of gray-level image $I_{(p\times q)}$ is obtained.

3.2.2 M-GLCM

The GLCM can demonstrate the structural information of texture in spatial domain; however, the information is obtained at the single scale. In contrast, the wavelet analysis enables the decomposition of images into the approximation sub-images and detail images and thus helps to get more statistical features of texture than the single-scale feature, it is helpless for the analysis of structural information of froth images. In view of that, A M-GLCM is proposed in this paper for the sake of acquiring comprehensive and accurate information about froth texture.

The coefficient matrix of the approximation sub-image, $c_{k,m}^{j}$ and those of detail images, $d_{k,m}^{j,1}$, $d_{k,m}^{j,2}$, $d_{k,m}^{j,3}$, at each scale are worked out according to formula (2), and then

their gray-level is respectively mapped according to the following formula:

$$C_j'(k,m) = 255 \times \left(C_j(k,m) - c_{\min}\right) \Big/ \left(c_{\max} - c_{\min}\right) \tag{4}$$

In formula (4), k and m refer to the row value and column value of the matrix element; $c_{\min}$ and $c_{\max}$ represent the minimum and maximum values of all the elements in matrix C_j.

The coefficient matrices obtained after mapping are $c'^{j}_{k,m}$, $d'^{j,1}_{k,m}$, $d'^{j,2}_{k,m}$, $d'^{j,3}_{k,m}$, and then their gray-levels are quantized with a quantitative series of 8; at last, the spatial gray-level co-occurrence matrices of the four angles, 0°, 45°, 90° and 135°, $P_j(k',m')$ are respectively worked out.

3.3 Feature Extraction Based on M-GLCM

The second statistics from M-GLCM on various directions are obtained, which include energy, entropy, contrast ratio and correlation of Haralick features and their averages on each direction etc.

As follows (Haralick et al., 1973):

Secondary Moment (Energy)

$$E = \sum_{k'=0}^{L-1} \sum_{m'=0}^{L-1} [P_j(k',m')]^2 \tag{5}$$

Entropy

$$S = -\sum_{k'=0}^{L-1} \sum_{m'=0}^{L-1} P_j(k',m') \log P_j(k',m') \tag{6}$$

Contrast Ratio (Inertia Moment)

$$I = \sum_{k'=0}^{L-1} \sum_{m'=0}^{L-1} [(k'-m')^2 P_j(k',m')] \tag{7}$$

Correlation

$$C(d,\theta) = \frac{\sum_{k',m'} (k'-\mu_x)(m'-\mu_y) P_j(k',m' \mid d,\theta)}{\sigma_x \sigma_y} \tag{8}$$

Wherein:

$$\mu_x = \sum_{k'} k' \sum_{m'} P_j(k',m' \mid d,\theta)$$

$$\mu_y = \sum_{m'} m' \sum_{k'} P_j(k',m' \mid d,\theta)$$

$$\sigma_x = \sum_{k'} (k'-\mu_x)^2 \sum_{m'} P_j(k',m' \mid d,\theta)$$

$$\sigma_y = \sum_{m'} (m'-\mu_y)^2 \sum_{k'} P_j(k',m' \mid d,\theta)$$

4. ONLINE CONDITION RECOGNITION

Fig.6 shows the online condition recognition system based on M-GLCM and Extreme Learning Machine (ELM). ELM is proposed by Huang.et al.(2004) for generalized single hidden layer feed-back networks (SLFNs) which can randomly chooses the input weights and analytically determines the output weights of SLFNs. It can provide better generalization performance at extremely high learning speed and has been successfully applied in both classification and regression applications.

4.1 Offline classification

After collection of froth videos in different conditions from copper flotation site, multi-scale texture features of each image are obtained offline according to the proposed method in this paper. Finally, these features are input to an ELM to analytically learn an optimal model and offline classification rate are obtained at the same time.

4.2 Online recognition

After training, the ELM is ready to recognize different conditions. Real-time images from the froth videos at a period are acquired. M-GLCM features of these images are calculated and input to the trained ELM. Finally, the recognition results of the ELM are presented.

.

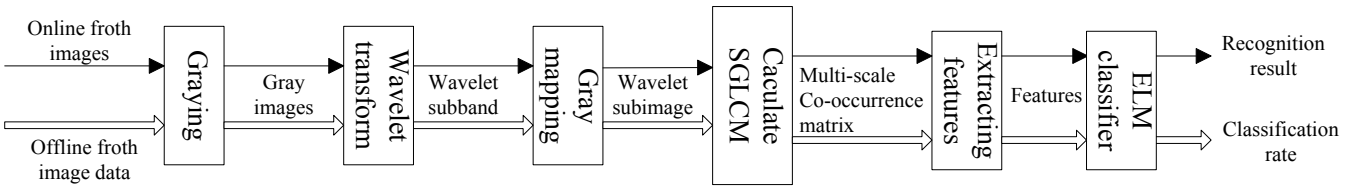

Fig.6 Block diagram for condition recognition based on M-GLCM

5. EXPERIMENT AND ANALYSIS

Froth videos are obtained in a steady state of the copper flotation site. Table.1 shows the feed ore characteristics of copper flotation processes.

5.1 Texture Features Extraction

5.1.1 Stability Analysis of M-GLCM Texture Features in the Same Working Condition

Table.1 List of process parameters

	Feed grade	Pulp concentration	Ph	Slurry particle size
min	0.85	25%	10	65%
max	1.12	32%	12	70%

An important characteristic of feature extraction is its stability. In working condition recognition, the effectiveness of feature extraction method is supposed to ensure that features extraction from different images in the same working condition are relatively stable. In the experiment, the froth video of normal working condition is acquired from the flotation site by the system shown in Fig.1, from which 15 frames of images are obtained. According to the proposed method, energy, entropy, contrast ratio and correlation of each image are extracted. Fig.7 shows the texture features on 135° direction of the M-GLCM.

As shown in Fig.7, these features from the froth video in that condition keep a relatively good stability and do not fluctuate greatly in different periods. To evaluate the stability quantitatively, the 3σ edit rule is applied to each kind of features and the results show that all (100%) of the values lie within three standard deviations of the mean of features respectively. The results prove that the texture features extracted by proposed M-GLCM method in this paper enjoy a good stability.

5.1.2 Separability Analysis of M-GLCM Texture Features in different Working Conditions

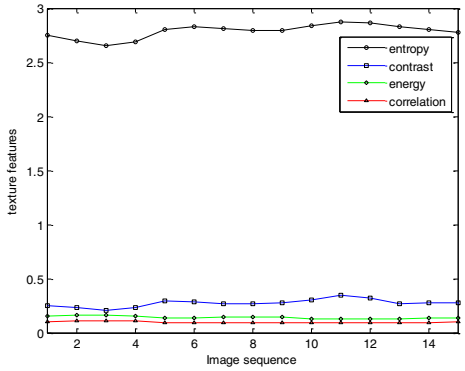

Fig.7 Texture features extracted by M-GLCM under normal condition

Another important characteristic of feature extraction is its separability. In working condition recognition, the effectiveness of feature extraction method is supposed to ensure that features extracted from froth images in different conditions have good separability. Froth images are acquired from videos of three different conditions as mentioned above. According to the proposed method, features include energy, entropy, contrast ratio and correlation on four directions are extracted from each image. Fig.8 shows the texture features on 135° direction of the M-GLCM.

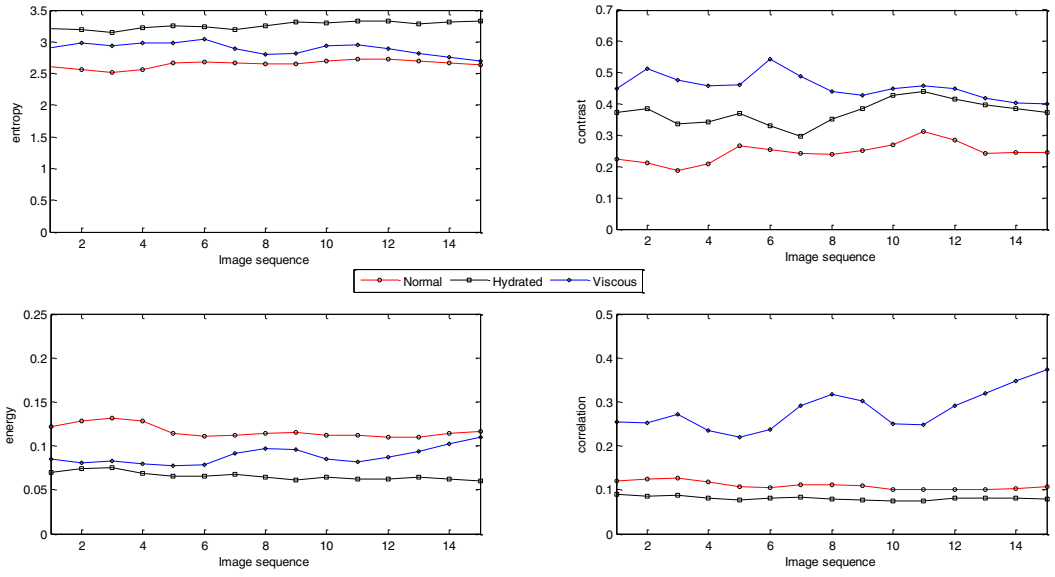

Fig.8 Texture features extracted by M-GLCM under different conditions

A one-way between subjects ANOVA is conducted to compare the effect of different conditions on features. Take the energy feature as an example, there is a significant effect of kinds of conditions on the level of energy at the $p<0.5$ level for the three conditions [$F(2, 14) = 4.162$, $p = 0.022$]. Post hoc comparisons using the Tukey HSD test indicate that the mean score of energy for the normal condition ($M = 0.127$, $SD = 0.006$) is significantly different from the viscous condition ($M = 0.088$, $SD = 0.009$). Also, the hydrated condition ($M = 0.073$, $SD = 0.005$) is significantly

different from normal and viscous conditions. Taken together, these results suggest that different conditions really do have an effect on the high levels of features. Therefore, the texture features of different conditions extracted from the M-GLCM enjoy a good separability. As a result, the distribution of texture features can help to effectively classify different froth images and thus recognize different working conditions.

5.2 Offline Classification of Copper Flotation Conditions

A total of 9 froth videos of different working conditions are acquired through the system as shown in Fig.1, among which 3 are of normal condition and 6 are of fault condition. The sampling frequency is 7.5 frames per second. The first ten frames of images from each video are used for training, while the last five frames are used for testing. In this way, there are a total of 90 training samples and 45 testing samples.

First, as for each froth image, the texture features on different directions from the M-GLCM are extracted. Based on these features, froth images are classified into three types with the ELM, namely, the normal, hydrated and viscous images. The training accuracy rates reach to almost 100% when the sigmoid function is choose as activation function, and the hidden neurons are set to 20 in the ELM . Table.2 shows the test accuracy rate of classification.

Table.2 Accuracy rate of classification for different M-GLCM features

	Energy	Entropy	Contrast Ratio	Correlation	Four Features
0°	0.7333	0.8000	0.8667	0.9333	0.8222
45°	0.8444	0.8667	0.7111	0.8667	0.8000
90°	0.6000	0.9111	0.5556	0.6667	0.5556
135°	0.8444	0.9333	0.9556	0.9556	0.9556
Average	0.8667	0.8667	0.9556	0.8667	0.8667

As shown in Table.2, texture features of a 135° angle in the M-GLCM have a relatively high accuracy rate of classification. Therefore, those features are selected as the final feature vector and adopted in the comparative experiment with features from GLCM and energy values from wavelet transform respectively, in which the Extreme Learning Machine is used to classify the froth images into three types, the normal, viscous and hydrated one. As to the GLCM, the accuracy rates of each direction are almost the same , so we also choose the features of 135° as the final feature vector .The result is shown in Table.2.

Table.3 Accuracy rate of classification for features extracted by different methods

	Wavelet Transform	GLCM	M-GLCM
Classification Accuracy Rate	0.7333	0.8222	0.9778

Table.3 shows that features extracted by M-GLCM enjoy the highest accuracy rate of classification, compared with the energy features from wavelet transform and those from the GLCM. In this way, it is clear that the texture features of froths can be better represented by M-GLCM.

5.3 Online Recognition of Fault Condition in Copper Flotation Process

The online monitoring of flotation conditions is carried out by online extraction of texture features from M-GLCM. First, according to the procedures in Section 4, the M-GLCM texture features of certain froth image are obtained online in real time. Then based on the trained ELM, the working conditions for the real-time froth images are determined. As demonstrated in Fig.9, we can easily know that the current working condition is normal condition.

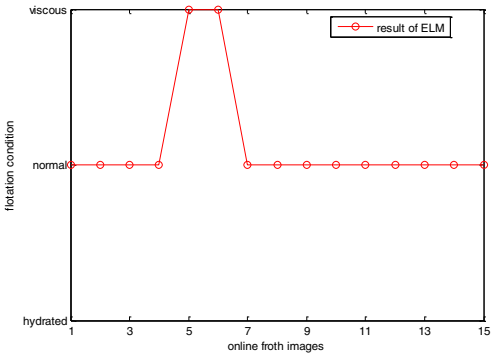

Fig.9 Online recognition result of ELM

6. CONCLUSION

This paper aimed at fault condition recognition of copper flotation based on froth image texture analysis. A method based on the M-GLCM for feature extraction is proposed. Texture features extracted by M-GLCM contain textural information of original images at different scales, which perform better than single-scale spatial features as well as traditional wavelet transform features. Results from both offline classification and online detection indicate that the texture features from the M-GLCM can recognize accurately the fault condition on copper flotation site in real time. However, more process variables should be taken into account to realize optimal control of the whole system, e.g. air flow rate, feed grade, reagent addition. And our future work will focus on that and the application of the method to wider range of external operating

conditions.

ACKNOWLEDGMENTS

This work is supported by the key Program of the National Nature Science Foundation of China under Grant 61273169, National Nature Science Foundation of China under Grant 61134006 and the National Key Technology R&D Program under Grant 2012BAK09B04.

REFERENCES

Moolman D.W., Eksteen J.J., Aldrich C. (1996). The significance of flotation froth appearance for Machine Vision Control *Mineral Process*, 48:135—158.

Aldrich C., Marais C., Shean B.J., Cilliers J.J. (2010). Online monitoring and control of froth flotation systems with machine vision: A review. *International Journal of Mineral Processing*, 96(4):1-13.

Yang C.H., Zhou K.J., Mu X.M., Gui W.H. (2009). Froth color and size measurement method for flotation based on computer vision. *Chinese Journal of Scientific Instrument*, 30(4):717-721.

Xu C.H., Gui W.H., Yang C.H. (2012). Flotation process fault detection using output PDF of bubble size distribution. *Minerals Engineering*, 26:5-12.

Lin Y.Q., Yang C.H., He M.F., Gui W.H. (2013). Fault condition detection for sulfur flotation process based on texture unit distribution. *Computing Technology and Automation*, 32(1):28-31.

Yang C.H., Ren H.F., Gui W.H., Yan F., Tang Z.H. (2011). Performance recognition using texture credit distributed SVM for froth flotation process. *Chinese Journal of Scientific Instrument*, 32(10): 2205-2209.

Haralick R.M., Shanmugam K., Dinstein I. (1973). Textural features for image classification. *IEEE Transactions on Systems, Man, and Cybernetics*, 3(6):610-621.

Mallat S.G. (1989). A theory for multiresolution signal decomposition: the wavelet representation. *IEEE Transactions on pattern Analysis and Machine Intelligence*, 11(7):674-693.

Wang J.S., Gao X.W., Zhang Y. (2010). Research on recognizing flotation states based on image texture features and multi-layer SVMs, *Control and Decision*, 25(10).

Ren H.F., Yang C.H., Zhou X., GUI W.H., YAN F. (2011). Froth image feature weighted SVM based working condition recognition for flotation process. *Journal of Zhejiang University*, 45(12): 2115-2119.

Liu L., Kuang G.Y. (2009). Overview of image textural feature extraction methods. *Journal of Image and Graphics*, 14(4):622-635.

Liu J.P., Gui W.H., Mu X.M., Tang Z.H., Li J.Q. (2010). Flotation froth image texture feature extraction based on Gabor wavelets, *Chinese Journal of Scientific Instrument*, 31(8):1769·1775.

Gianni B., Patrick P. Jr., Jayson T. Jr., Duchesne C., et al. (2006).Application of numerical image analysis to process diagnosis and physical parameter measurement in mineral processes-Part I: Flotation control based on froth textural characteristics. *Minerals Engineering*, 3(19):734-747.

Zhong H., Yang X.M., Jiao L.C. (2011). Texture Classification Based on Multiresolution Co-occurrence Matrix. *Journal of Computer Research and Development*,48(11).

Huang G B, Zhu Q Y, Siew C K.(2004). Extreme learning machine: a new learning scheme of feedforward neural networks. *Neurocomputing*, 2(2): 985-990.